Journal of Crystal Growth 427 (2015) 94–98

Contents lists available at ScienceDirect

Journal of Crystal Growth

journal homepage: www.elsevier.com/locate/jcrysgro

Floating zone growth of Ba-substituted ruthenate $Sr_{2-x}Ba_xRuO_4$

Z.W. Li [a,*], C.-F. Liu [a,b], M. Skoulatos [c], L.H. Tjeng [a], A.C. Komarek [a,*]

[a] Max-Planck-Institute for Chemical Physics of Solids, Nöthnitzer Str. 40, 01187 Dresden, Germany
[b] Department of Electrophysics, National Chiao Tung University, HsinChu 30100, Taiwan
[c] Paul Scherrer Institute, LNS, 5232 Villigen, Switzerland

ARTICLE INFO

Article history:
Received 8 April 2015
Received in revised form
7 July 2015
Accepted 8 July 2015
Communicated by R.S. Feigelson
Available online 16 July 2015

Keywords:
B1. Ruthenium oxide
B1. Ruthenate
A2. Floating zone
A2. Single crystal growth
B2. Oxide superconducting materials
B2. Superconducting materials
B2. Unconventional superconductor

ABSTRACT

We report on the exploration to synthesize $Sr_{2-x}Ba_xRuO_4$, the large volume variant of the unconventional superconductor Sr_2RuO_4. We have succeeded in growing single crystals for x-values up to 0.4 by making use of the traveling solvent floating zone method. The quality of the obtained crystals is confirmed by X-ray and neutron diffraction measurements and the properties of these Ba-substituted ruthenates were studied with magnetic and electrical transport measurements.

1. Introduction

Single-layered perovskite ruthenates have attracted enormous interest since the discovery of superconductivity in Sr_2RuO_4 30 years ago [1]. Like other unconventional superconductors, it was also found that the superconductivity in Sr_2RuO_4 is in close proximity to magnetic instabilities [2–5]. Rather unique compared to other superconductors with s-wave or d-wave pairing, Sr_2RuO_4 is believed to exhibit spin-triplet p-wave pairing [5–7]. It has been proposed that ferromagnetic (FM) spin fluctuations play a key role in the pairing mechanism of Sr_2RuO_4. Intense research activities have been focused on the search for FM spin fluctuations in this compound and accumulating evidence has been acquired which point to a coexistence of both weak FM and short-ranged incommensurate antiferromagnetic (AFM) type correlations [2,3,8]. Further interest has been generated from the investigation of the Ca-substituted Sr_2RuO_4 system (substitution of Sr by smaller Ca ions) which exhibits a rich phase diagram [9–11]. Finally, the pure Ca_2RuO_4 compound is shown to be a Mott insulator that orders antiferromagnetically below 110 K [9] and FM type cluster spin glass states exists in a large doping range [4]. The research was also extended to doping elements both at the Sr-site (with La, etc.) and at the Ru-site (with Ti, Co, Mn, etc.) site to enhance FM or AFM fluctuations or even trigger static orders of either type [12–14]. Substitution or doping at the Sr site has the advantage that it leaves the Ru–O plane intact. Nevertheless, apart from the very well-studied Ca-substituted system, there is relatively less work using other substitution or doping elements, especially those that can enlarge the volume of the unit cell without altering the Ru–O planes [15]. This is in particular interesting since the superconducting transition temperature of Sr_2RuO_4 can be enhanced strongly using strain [16]. In this work, we report on the growth of high quality and large volume single crystals of $Sr_{2-x}Ba_xRuO_4$ ($0.05 \leq x \leq 0.4$). The quality and physical properties of our crystals are characterized by X-ray and neutron diffraction, magnetic and electrical transport measurements.

2. Experimental procedure

In an initial step polycrystalline $Sr_{2-x}Ba_xRu_{1+y}O_4$ powders (with $y \lesssim 0.15$) were prepared from $SrCO_3$ (99.99%, Alfa Aesar), $BaCO_3$ (99.95%, Alfa Aesar) and RuO_2 (99.9%, Alfa Aesar). The powders were thoroughly ground followed by traditional solid-state reaction at 1100 °C for 48 h in air with intermediate grindings. The resulting powder was packed into latex tubes and pressed into rods of ~6 mm in diameter and ~14 cm in length under ~100 MPa hydrostatic pressure and, then, sintered again at

* Corresponding authors.
E-mail addresses: Zhiwei.Li@cpfs.mpg.de (Z.W. Li), Komarek@cpfs.mpg.de (A.C. Komarek).

http://dx.doi.org/10.1016/j.jcrysgro.2015.07.011
0022-0248/

1100 °C to make a dense feed rod. The Ru-excess y in the feed rod acts as self-flux and a compensation to the evaporation of RuO_2 (which is heavily evaporating during the growth procedure), and, is essential for the successful growth of large crystals of ruthenates [17,18]. In the next step single crystals were grown from these polycrystalline feed rods by the floating zone technique using a single crystal of the same composition as a seed. The atmosphere during the crystal growth was maintained in a high pressure optical mirror furnace (High Pressure Crystal Growth Furnace, Scientific Instrument Dresden GmBH) that is able to reach gas pressures up to 150 bar using a mixture of Ar and O_2 with a ratio of 9:1 and with a flowing rate of 1 l/min. The seed crystal and the feed rod were counter-rotated at 30 rpm and a growth speed of 15–30 mm/h was used during crystal growth.

Powder X-ray diffraction measurements have been performed with a 2θ step of 0.005° on powders ground from our single crystals using Cu $K_{\alpha 1}$ radiation of a laboratory X-ray source. The magnetic properties of our single crystals were measured using a SQUID magnetometer (MPMS, Quantum Design). The neutron data was collected at the cold neutron triple-axis spectrometer RITA-II at the Paul Scherrer Institute, Villigen, Switzerland, using a neutron wavelength of ~4.05 Å corresponding to $k_i = k_f = 1.55$ Å^{-1}. Electrical transport properties of our crystals were measured using a physical property measurement system (PPMS, Quantum Design). Samples were cut into bars with typical dimensions $\sim 1 \times 1 \times 2$ mm^3. Four probe contacts were made by connecting Au wires using silver paste.

3. Results

$Sr_{2-x}Ba_xRuO_4$ single crystals with several centimeters in length and ~5–6 mm in diameter could be obtained within the Ba-substitution range $0.05 \leq x \leq 0.4$. Attempts to grow doping levels higher than $x > 0.4$ always end with small crystals grown together with other impurity phases. One possible reason for this observation could be that one enters the regime of a miscibility gap at higher Ba-substitution $x > 0.4$.

The growth direction was determined by X-ray Laue diffraction to be the tetragonal [110]-direction and the facets, which can be readily seen from Fig. 1(a)–(g), are the (001) plane of the single crystal. The sharp X-ray Laue diffraction pattern along the [001]-axis of a $Sr_{2-x}Ba_xRuO_4$ ($x=0.4$) crystal shown in Fig. 1(h) confirms the sample quality of our as-grown single crystals.

Finally, long scans across the whole length of the single crystal and from different sides have been performed with our real-time Laue camera. These real-time Laue scans indicate only one single domain along the entire growth direction of our single crystals for all investigated sides of each crystal, thus, confirming the single crystallinity of our crystals.

3.1. Characterization

The phase purity and lattice parameters of the grown crystals were determined at room temperature by powder X-ray diffraction (PXRD). A typical PXRD pattern for $Sr_{2-x}Ba_xRuO_4$ ($x=0.4$) crystal is shown in Fig. 2(a). It was possible to describe the crystal structure with space group I4/mmm as for the undoped parent compound Sr_2RuO_4 [1]. The two broad features marked with ∗, which is common for all the PXRD pattern measured in our laboratory, originate from the sample holder. All the other peaks can be indexed and refined properly by Rietveld refinement, indicating phase purity. The Ba-substitution dependence of the a and c lattice parameters is plotted in Fig. 2(b). The linear increase of a and c with Ba-substitution level x is basically following Vegard's law and indicates the successful substitution of the Strontium by the larger Barium atom in the $Sr_{2-x}Ba_xRuO_4$ series. Also a linear fit of the data yields extrapolated values of $a_0=3.8704(7)$ Å and $c_0=12.745(4)$ Å for $x = 0$ which is very close to reported values ($a_0=3.87$ Å and $c_0=12.74$ Å) for the parent compound Sr_2RuO_4 [1].

Furthermore, we have performed inductively coupled plasma optical emission spectrometry (ICP-OES) measurements in order to, finally, confirm the successful Ba-substitution in our single crystals. In Fig. 3 the resulting measured Ba-concentration obtained from our ICP-OES measurements is plotted as a function of the nominal Ba-substitution of each single crystal. As can be seen, our Ba-substituted single crystals are essentially stoichiometric.

Fig. 4 shows the rocking curves of in total ~50 g co-aligned single crystals of $Sr_{2-x}Ba_xRuO_4$ ($x=0.4$) measured by means of neutron diffraction on a cold triple-axis-spectrometer. The co-aligned crystal ensemble used for this measurement is shown in the inset of Fig. 4(a). In total, 14 single crystals of $Sr_{1.6}Ba_{0.4}RuO_4$ were co-aligned on an aluminium sample holder with the crystallographic c-axis perpendicular to the neutron beam, see the inset of Fig. 4(a). The full scan across two of the four-fold peaks (200) and (020) that is plotted in Fig. 4(a) clearly indicates the absence of crystal grains from other domains in our entire crystal ensemble. Fig. 4(b and c) shows the fits of the (020) and (200) reflections with a Gaussian distribution. The full width at half maximum (FWHM) for these two peaks obtained from Gaussian fits amounts to 0.982° and 0.875°. The relative small values of the FWHM (note that we have co-aligned 14 pieces of crystals) prove both the good mosaicity of our single crystals and a proper co-alignment of the entire crystal ensemble.

3.2. Magnetic and transport properties

In Fig. 5, we present the zero-field-cooled (ZFC) and field-cooled (FC) magnetic susceptibilities $\chi \equiv M/H$ of a $Sr_{2-x}Ba_xRuO_4$ ($x=0.4$) single crystal as a function of temperature measured in a magnetic field of $H=0.5$ T applied along the [110]-direction ($\chi_{[110]}$, $\mathbf{H} \| [110]$) and along the [001]-direction ($\chi_{[001]}$, $\mathbf{H} \| [001]$). As can be seen, χ shows an anisotropy with $\chi_{[001]} > \chi_{[110]}$ over the whole measured temperature range. At high temperatures, both $\chi_{[001]}$ and $\chi_{[110]}$ are characterized by a weakly temperature dependent component, $\chi_{[001]}(300\text{ K}) = 7.6 \times 10^{-4}$ cm^3/mol and $\chi_{[110]}(300\text{ K}) = 4.6 \times 10^{-4}$ cm^3/mol. These magnetic properties resemble the Pauli-paramagnetic properties of the parent compound Sr_2RuO_4 [1] which is different from the observations in Ca-substituted compounds where χ shows a Curie–Weiss-like behavior [9,10]. Interestingly, at low temperatures, χ shows a steep upturn for both measured directions which shows a directional dependence. The anisotropy of this ferromagnetic signal that appears only at lowest temperature can be seen best in the magnetization curves shown in Fig. 6. Whereas the magnetization curve is almost linear for the [110]-direction (in-plane) it exhibits a ferro-/ferrimagnetic character in the [001]-direction (out-of plane).

The in-plane and out-of-plane resistivities of a $Sr_{2-x}Ba_xRuO_4$ ($x=0.4$) are shown in Fig. 7. The corresponding residual resistivity ratio (RRR) is calculated to be $RRR_{[110]} \equiv \rho_{[110]}(300\text{ K})/\rho_{[110]}(2\text{ K}) = 17.6$ and $RRR_{[001]} \equiv \rho_{[001]}(300\text{ K})/\rho_{[001]}(2\text{ K}) = 9.2$. Similar to the parent compound Sr_2RuO_4, the out-of-plane resistivity $\rho_{[001]}$ shows a crossover from non-metallic to metallic temperature-behavior with a broad maximum at $T_M \sim 140$ K [1]. On the other hand, the in-plane resistivity measured with electric current along [110] direction, $\rho_{[110]}$, shows metallic behavior in the whole measured temperature range (only a small change in the slope of $\rho_{[110]}$ is also visible in that temperature range). I.e. at high temperatures, $Sr_{1.6}Ba_{0.4}RuO_4$ exhibits only in-plane a metallic temperature dependence of ρ, whereas, at low temperatures, the crystal shows a metallic temperature dependence of ρ in all three crystallographic directions.

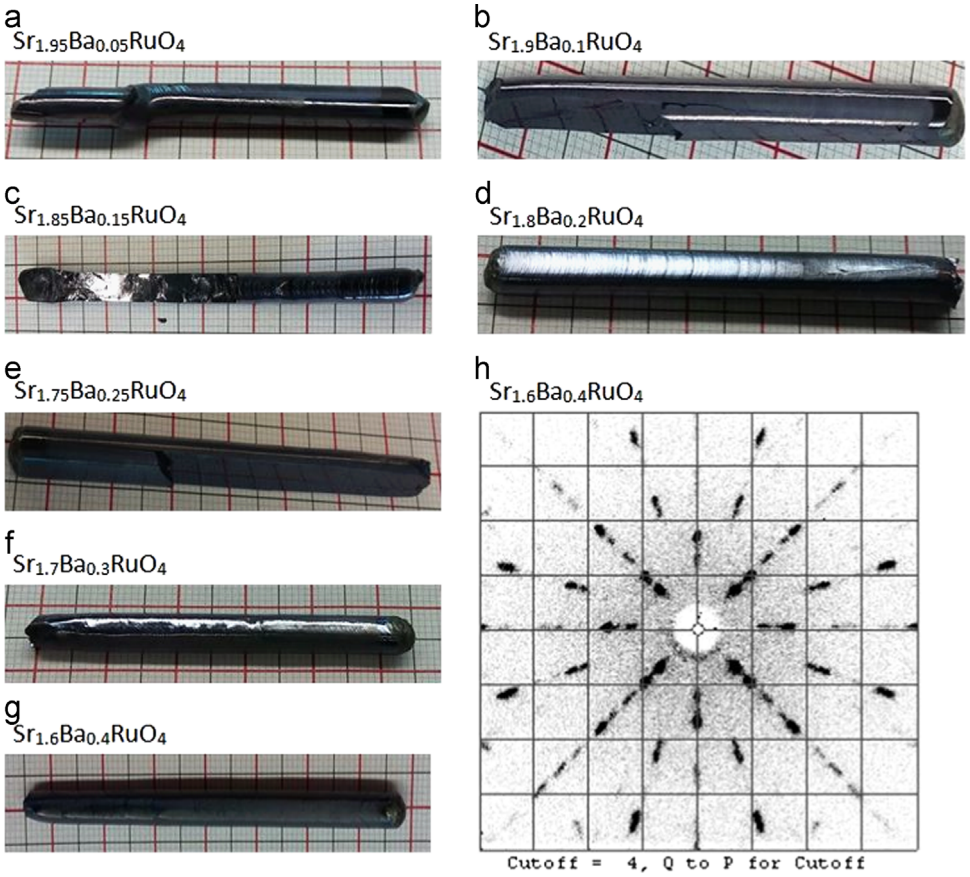

Fig. 1. (a)–(g) Pictures of the as-grown crystals of $Sr_{2-x}Ba_xRuO_4$ with indicated x values. (h) A X-ray Laue pattern along [001]-direction for the crystal of $Sr_{1.6}Ba_{0.4}RuO_4$ measured with our real-time Laue camera.

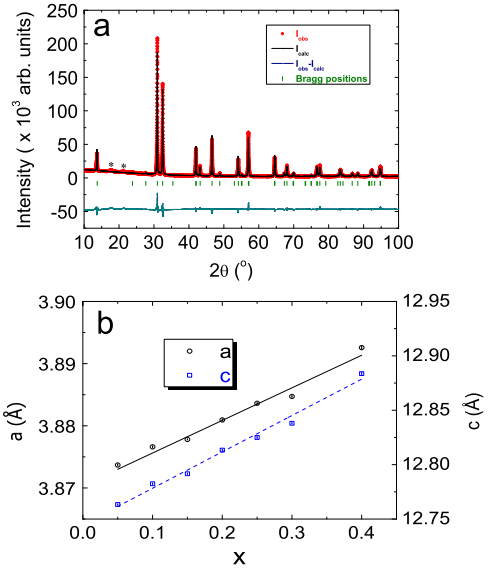

Fig. 2. (a) Room-temperature powder X-ray diffraction pattern of a powder sample of $Sr_{2-x}Ba_xRuO_4$ ($x=0.4$) obtained from crushed single crystals. A Rietveld refinement calculated with space group I4/mmm is able to describe the data properly (the two broad features marked with ∗ originate from the sample holder). (b) Doping dependence of lattice parameters of $Sr_{2-x}Ba_xRuO_4$.

The absolute value of $\rho_{[001]}$ and $\rho_{[110]}$ at 300 K is $2.9\times10^{-2}\,\Omega\,\mathrm{cm}$ and $2.1\times10^{-2}\,\Omega\,\mathrm{cm}$, respectively, which gives an anisotropy ratio of $\rho_{[001]}/\rho_{[110]}\sim1.4$. This is much smaller than that of the Sr_2RuO_4 parent compound which amounts to ~220 [1].

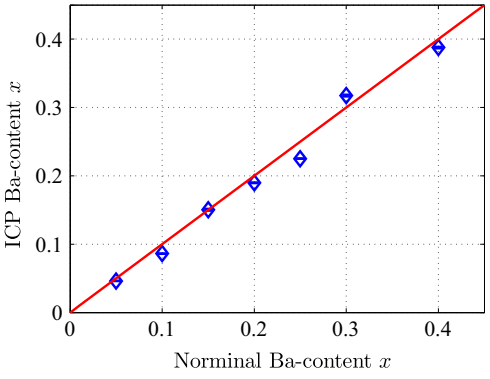

Fig. 3. The Ba-concentration in our $Sr_{2-x}Ba_xRuO_4$ single crystals as derived from ICP-OES measurements. The values measured by ICP-OES are plotted versus the nominal Ba-concentration of each single crystal.

Note that the out-of-plane resistivity for Sr_2RuO_4 is roughly $\sim4\times10^{-2}\,\Omega\,\mathrm{cm}$. Fig. 7(b) shows the decrease of the anisotropy ratio as a function of Ba-content. This indicates that Ba-substitution greatly increases the in-plane resistivity. For the Ca-substituted $Sr_{2-x}Ca_xRuO_4$ system, the in-plane resistivity only slightly changes with Ca doping and remains metallic in a large doping range ($0<x<1.8$) while the out-of-plane resistivity changes significantly upon Ca doping and they finally become Mott insulating for both measured directions in the vicinity of the pure Ca_2RuO_4 [9,10]. But whereas octahedral tilts are induced by doping of smaller Ca-ions in Sr_2RuO_4, the doping with larger Ba-ions only induces an increase of the unit cell volume. No

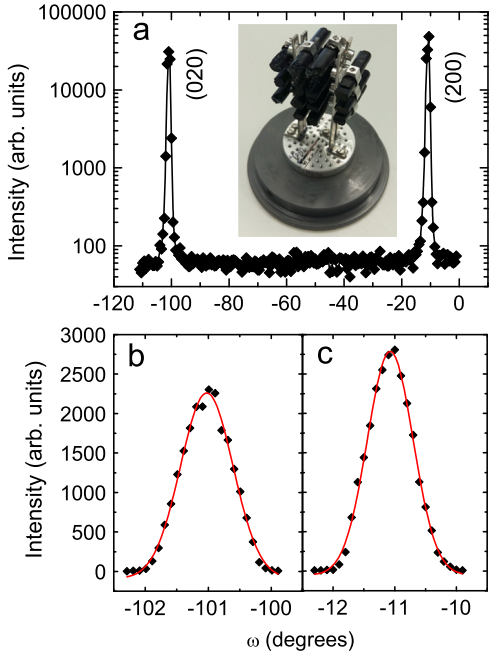

Fig. 4. Neutron rocking curves of ~50 g co-aligned single crystals of $Sr_{2-x}Ba_xRuO_4$ ($x=0.4$). (a) A large scan across two of the four-fold peaks (200) and (020) is shown. The measured crystal ensemble is shown in the inset. (b and c) A Gaussian fit to the (020) and (200) reflections yields a full width at half maximum (FWHM) which amounts to 0.982° and 0.875° respectively.

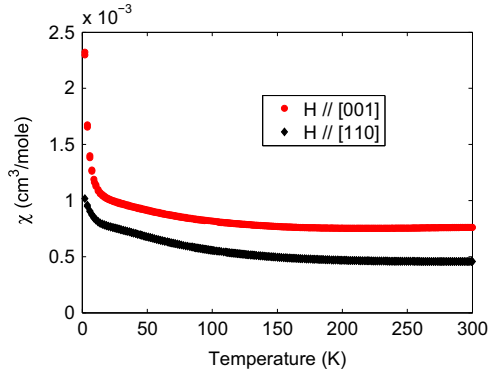

Fig. 5. Zero-field-cooled (ZFC) and field-cooled (FC) magnetic susceptibility χ of a $Sr_{2-x}Ba_xRuO_4$ ($x=0.4$) single crystal as a function of temperature measured in a magnetic field of $H=0.5$ T applied along the [110]-direction ($\chi_{[110]}$, $\mathbf{H}\|[110]$) and along the [001]-direction ($\chi_{[001]}$, $\mathbf{H}\|[001]$).

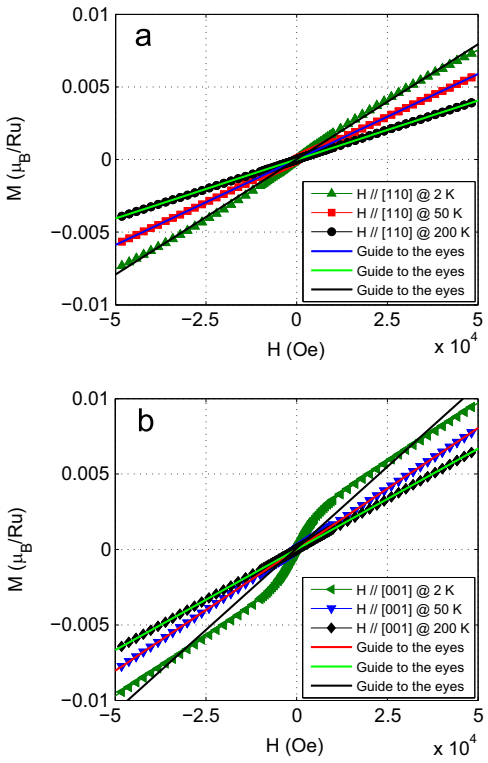

Fig. 6. Magnetization curves along the [110]-direction and along the [001]-direction measured on the same sample at $T=2$, 30 and 200 K. The magnetization curve in [001]-direction measured at 2 K clearly deviates from a linear field-dependence.

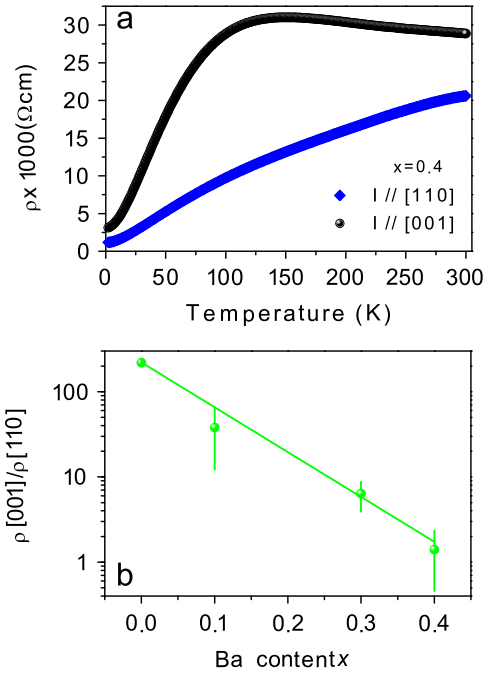

Fig. 7. (a) The resistivity ρ of $Sr_{2-x}Ba_xRuO_4$ ($x=0.4$) measured using an excitation current of $I=5$ mA along the [110]-direction ($\rho_{[110]}$, $\mathbf{I}\|[110]$) and along the [001]-direction ($\rho_{[001]}$, $\mathbf{I}\|[001]$). (b) The anisotropy ratio $\rho_{[001]}/\rho_{[110]}$. The value for the Sr_2RuO_4 parent compound was taken from Ref. [1]. Error bars are systematic errors due to (maximum possible) uncertainties of the sample dimensionality.

octahedral tilts are induced by Ba-substitution. Our observations in floating zone grown single crystals are in contrast to observations in older powder studies [15]. Our observed increase of the in-plane resistivity with increasing Ba-content may be caused by local scattering processes associated with the introduction of the huge Ba-ions. This may also be accompanied by nano phase separation which was recently found to play an important role for several transition metal oxides that cannot be entirely understood based on homogenous phases [19–24].

4. Conclusion

In conclusion, we have succeeded in growing single crystals of $Sr_{2-x}Ba_xRuO_4$ in the doping range $0.05 \le x \le 0.4$ by the floating zone technique. The availability of high quality and large volume crystals will enable future studies of the other side of the $Sr_{2-x}A_x^{2+}RuO_4$ phase diagram such as inelastic neutron scattering experiments where a large sample volume is required. Although no octahedral tilts are induced by Ba-substitution we still have indications for the introduction of more localizing properties

induced by Ba-substitution as indicated by the increased in-plane resistivity compared to the out-of-plane resistivity in $Sr_{1.6}Ba_{0.4}RuO_4$. Finally, we observe a direction-dependant ferro-/ferri-magnetic signal or contribution in magnetization measurements of $Sr_{2-x}Ba_xRuO_4$ that appears at lowest temperatures.

Acknowledgments

We thank the team of H. Borrmann for powder X-ray diffraction measurements and the team of G. Auffermann for ICP measurements. This work is partially based on experiments performed at the Swiss spallation neutron source SINQ, Paul Scherrer Institute, Villigen, Switzerland.

References

[1] Y. Maeno, H. Hashimoto, K. Yoshida, S. Nishizaki, T. Fujita, J.G. Bednorz, F. Lichtenberg, Nature 372 (1994) 532.
[2] Y. Sidis, M. Braden, P. Bourges, B. Hennion, S. NishiZaki, Y. Maeno, Y. Mori, Phys. Rev. Lett. 83 (1999) 3320.
[3] M. Braden, Y. Sidis, P. Bourges, P. Pfeuty, J. Kulda, Z. Mao, Y. Maeno, Phys. Rev. B 66 (2002) 064522.
[4] J.P. Carlo, T. Goko, I.M. Gat-Malureanu, P.L. Russo, A.T. Savici, A.A. Aczel, G. J. MacDougall, J.A. Rodriguez, T.J. Williams, G.M. Luke, C.R. Wiebe, Y. Yoshida, S. Nakatsuji, Y. Maeno, T. Taniguchi, Y.J. Uemura, Nat. Mater. 11 (2014) 323.
[5] J.A. Duffy, S.M. Hayden, Y. Maeno, Z. Mao, J. Kulda, G.J. McIntyre, Phys. Rev. Lett. 85 (2000) 5412.
[6] G.M. Luke, Y. Fudamoto, K.M. Kjima, M.I. Larkin, J. Merrin, B. Nachumi, Y. J. Uemura, Y. Maeno, Z.Q. Mao, Y. Mori, H. Nakamura, M. Sigrist, Nature 394 (1998) 558.
[7] J. Xia, Y. Maeno, P.T. Beyersdorf, M.M. Fejer, A. Kapitulnik, Phys. Rev. Lett. 97 (2006) 167002.
[8] T. Imai, A.W. Hunt, K.R. Thurber, F.C. Chou, Phys. Rev. Lett. 81 (1998) 3006.
[9] S. Nakatsuji, Y. Maeno, Phys. Rev. Lett. 84 (2000) 2666.
[10] S. Nakatsuji, Y. Maeno, Phys. Rev. B 62 (2000) 6458.
[11] P. Steffens, O. Friedt, Y. Sidis, P. Link, J. Kulda, K. Schmalzl, S. Nakatsuji, M. Braden, Phys. Rev. B 83 (2011) 054429.
[12] M. Braden, Q. Friedt, Y. Sidis, P. Bourges, M. Minakata, Y. Maeno, Phys. Rev. Lett. 88 (2002) 197002.
[13] N. Kikugawa, A.P. Mackenzie, C. Bergemann, R.A. Borzi, S.A. Grigera, Y. Maeno, Phys. Rev. B 70 (2004) 060508(R).
[14] J.E. Ortmann, J.Y. Liu, J. Hu, M. Zhu, J. Peng, M. Matsuda, X. Ke, Z.Q. Mao, Sci. Rep. 3 (2013) 2950.
[15] K. Chandrasekaran, R. Vijayaraghavan, U.V. Varadaraju, Mater. Chem. Phys. 56 (1998) 63–69.
[16] C.W. Hicks, D.O. Brodsky, E.A. Yelland, A.S. Gibbs, J.A.N. Bruin, M.E. Barber, S. D. Edkins, K. Nishimura, S. Yonezawa, Y. Maeno, A.P. Mackenzie, Science 344 (2014) 283–285.
[17] Z.Q. Mao, Y. Maeno, H. Fukazawa, Mater. Res. Bull. 35 (2000) 1813.
[18] R.S. Perry, Y. Maeno, J. Cryst. Growth 271 (2004) 134.
[19] M. Fratini, N. Poccia, A. Ricci, G. Campi, M. Burghammer, G. Aeppli, A. Bianconi, Nature 466 (2010) 841–844.
[20] N. Poccia, A. Ricci, G. Campi, M. Fratini, A. Puri, D. Di Gioacchino, A. Marcelli, M. Reynolds, M. Burghammer, N. Lal Saini, G. Aeppli, A. Bianconi, Proc. Natl. Acad. Sci. 109 (2012) 15685–15690.
[21] A. Ricci, N. Poccia, G. Campi, F. Coneri, A.S. Caporale, D. Innocenti, M. Burghammer, M.v. Zimmermann, A. Bianconi, Sci. Rep. 3 (2013) 2383.
[22] Y. Drees, D. Lamago, A. Piovano, A.C. Komarek, Nat. Commun. 4 (2013) 2449.
[23] Y. Drees, Z.W. Li, A. Ricci, M. Rotter, W. Schmidt, D. Lamago, O. Sobolev, U. Rütt, O. Gutowski, M. Sprung, A. Piovano, J.P. Castellan, A.C. Komarek, Nat. Commun. 5 (2014) 5731.
[24] A. Ricci, N. Poccia, G. Campi, F. Coneri, L. Barba, G. Arrighetti, M. Polentarutti, M. Burghammer, M. Sprung, M.v. Zimmermann, A. Bianconi, New J. Phys. 16 (2014) 053030.